Title: Mass flow and velocity profiles in *Neurospora* hyphae: partial plug flow dominates intra-hyphal transport.

Running Title: Fungal mass flow

Contents Category: Physiology and Biochemistry

Aryan Abadeh and Roger R. Lew[1]
Department of Biology
York University
4700 Keele Street
Toronto, Ontario M3J 1P3 Canada

[1]Author for correspondence. Email: planters@yorku.ca; Telephone: (416) 736-5243; Fax: (416) 736-5698

Word counts: Summary (147 words); Text body (–ca 4500 words)
Number of figures: six
Number of tables: none

Microbiology 159:2386–2394
doi:10.1099/mic.0.071191-0

SUMMARY

Movement of nuclei, mitochondria and vacuoles through hyphal trunks of *Neurospora crassa* were vector-mapped using fluorescent markers and GFP tags. The vectorial movements of all three were strongly correlated, indicating the central role of mass (bulk) flow in cytoplasm movements in *N. crassa*. Profiles of velocity *versus* distance from the hyphal wall did not match the parabolic shape predicted by the ideal Hagen-Poiseuille model of flow at low Reynolds number. Instead, the profiles were flat, consistent with a model of partial plug flow due to the high concentration of organelles in the flowing cytosol. The intra-hyphal pressure gradients were manipulated by localized external osmotic treatments to demonstrate the dependence of velocity (and direction) on pressure gradients within the hyphae. The data support the concept that mass transport driven by pressure gradients dominates intra-hyphal transport. The transport is partial plug flow due to the organelles in the cytosol.

INTRODUCTION

Fungal hyphae grow into new territories while forming an interconnected mycelium behind the colony edge where nutrients are actively absorbed to fuel continued growth. Intracellular hydrostatic pressure is the major driving force for cellular expansion of hyphae at the edge of the fungal colony (Lew, 2011). Behind the colony edge, nutrients are transported throughout the interconnected mycelium. The transport of nutrients can be measured with radioactive tracers, and has velocities in the range of 3–70 μm s^{-1} (Jennings, 1987). These velocities would result in translocation that is farther than could be expected for diffusion alone. In 60 sec, a protein with a diffusion coefficient of 7×10^{-11} m^2 s^{-1} would travel an average (bidirectional) distance of about 35 μm compared to 180–4200 μm for unidirectional nutrient translocation. With recent advances in imaging techniques, it is now clear that there is a highly complex network of translocation (Fricker et al., 2007) that adapts dynamically (Bebber et al., 2007). Some of the genes that affect translocation have been identified in *Neurospora crassa* (Simonin et al., 2012); the gene products function in hyphal fusions that create a cytoplasmic continuum. At a localized scale, cytoplasmic movement translocates cellular components acropetally from vegetative hyphae to the growing edge of the colony (Riquelme, 2002), and to developing aerial hyphae in conidia formation (Bleichrodt et al., 2013).

The driving force for translocation could be molecular motors or a trans-hyphal pressure gradient, or both (Lew, 2011). When silicon oil was injected into hyphae, it moved through the hyphae similarly to vacuoles. Since the silicon oil should not interact with molecular motors, the likely cause of movement was trans-hyphal pressure gradients (Lew, 2005). Taking advantage of the ability to express green fluorescent protein (GFP) in *N. crassa* (Freitag et al., 2004), Ramos-García et al. (2009) monitored the movement of nuclei labeled with GFP-tagged histone. Nuclei movement towards the growing edge of the colony was still observed in strains with mutations in microtubule-related motors (dyenin and kinesin) and after treatment of wildtype with disruptors of cytoskeleton, corroborating the idea that bulk flow is an important determinant of organelle movement. Genetic intermixing —in

which mass flow plays a primary role— has been directly imaged using nuclei labeled with DsRed or GFP (Roper et al., 2013). At least in Basidiomycetes, an alternative transport mode relies upon movement through the vacuole system (Darrah et al., 2006).

In this paper, we explore the nature of mass flow in hyphae in greater detail. We use dual-imaging of mitochondria and either nuclei or vacuoles to correlate their vectorial movement within hyphae. Profiles of velocity *versus* distance from the hyphal wall were constructed to test for known models of bulk flow at low Reynolds number (Cox and Mason, 1971). Experimental manipulations of external osmolarity were used to directly modify the trans-hyphal pressure gradients required to drive mass flow through the hyphal network. The results indicate that mass flow dominates cytoplasm movement. Due to the high density of organelles, the movement deviates from Hagen-Poiseuille flow and is better described as partial plug flow.

METHODS

Strain preparation and media. A GFP-tagged histone strain (rid Pccg-1-hH1^{+}-sgfp^{+}, FGSC 10174) was obtained from the Fungal Genetics Stock Center (School of Biological Sciences, University of Missouri, Kansas City, Missouri, USA) (McCluskey et al., 2010) and maintained on slants of Vogel's Minimal Medium (Vogel, 1956) plus 1.5% (w/v) sucrose and 2.0% (w/v) agar. The GFP-tagged histone strain was used to visualize the fluorescently labeled nuclei. For visualizing vacuoles, a his-3^{+}::Pccg-1::nca-2^{+}::sgfp^{+} (FGSC 10160) strain was used. This strain has a GFP tagged nca-2. Nca-2 is a calcium transporter that is found in both vacuoles and a tubular internal membrane network (Bowman et al., 2009). Movement of the internal network was difficult to track with GFP-nca-2 because of the small size of the fluorescent structures (movement could be observed qualitatively), but large vacuoles could be readily tracked.

For the dual imaging experiments —in which both mitochondria and nuclei (or vacuoles) velocities were measured— the mitochondria were labeled with MitoTracker Red FM (Invitrogen Molecular Probes, Catalog Number M22425). Conidia from the GFP-tagged strains were spread in a 2 cm streak along the edge of a 55 mm Petri dish containing OM plus 1% agar and grown overnight at 28ºC. OM contains [% w/v]: glucose [1], peptone [0.1], yeast extract [0.01], KH_2PO_4 [0.1], and $MgSO_4 \cdot 7H_20$ [0.03]; peptone and yeast extract were obtained from Difco. To label mitochondria, 2.5 ml of OM containing MitoTracker Red FM (final concentration 12 µM from a 2 mM stock in methanol) was pipetted into the Petri plates on top of the mycelium after overnight growth so that the fungi continued to grow submerged in the medium. To maximize loading with MitoTracker, the plates were incubated for another 5-6 hours at 28ºC in the dark (less loading was observed when the Petri plates were incubated at room temperature). The MitoTracker fluorescence intensity was strongest at the hyphal tips, presumably because of the highly polarized membrane potential of tip-localized mitochondria (Levina and Lew, 2006), but could be readily visualized in hyphal trunks behind the colony edge for tracking movement of the mitochondria.

Dual fluorescent imaging using the Confocal Microscope. To image the hyphae *in situ*, the culture plates were mounted directly on the microscope stage and a cover slip gently placed over the colony edge. Hyphal trunks were selected on the basis of noticeable cytoplasm movement and strong fluorescence intensity of the mitochondria. Fluorescence scanning was performed using an EC Plan-Neofluar ×100 oil immersion objective (N.A. 1.3) on a Fluoview 300 confocal system (Olympus Canada). The nuclei and vacuoles (GFP) were imaged with an excitation wavelength of 488 nm. The mitochondria (MitoTracker Red) were imaged with an excitation wavelength of 579 nm. For both, the emission wavelength was 622 nm. Only a region of interest of the selected hypha was imaged to minimize the time required for scanning. Time series of 120 images were acquired at 1-second intervals with Kalman filtering. The image stacks were analyzed using ImageJ (Rasband, 2012).

Quantifying organelle flow. For nuclei and vacuoles, it was relatively easy to track the movements of the organelles using ImageJ. Mitochondria fluorescence was not as discretely located, due to the pleiomorphic structure of the mitochondria (tubular to filamentous [Luck, 1963]). In all cases, the fluorescence images were digitally enhanced with linear contrast stretch and Gaussian filtering (1.5 pixel radius) in ImageJ to make organelle tracking easier (Fig. 1). For any given experiment, a sample size of 5–7 mitochondria and nuclei or vacuoles were selected in each digital image. Their movement along the hyphal trunk was tracked for three sequential images and their displacement (x-y coordinates) over the two 1-second intervals was recorded (Fig. 1). The x-y coordinates for the two 1-second intervals were converted to vectors of average velocity ($\mu m\ s^{-1}$) and direction (as an angle) using MATLAB. We did not document the zero velocities at the wall boundary because we expected that cytoskeleton effects would be more pronounced at the immobile wall and to avoid the complexities of boundary effects.

To analyze the correlations between velocity and direction for the mitochondria and nuclei or mitochondria and vacuoles, the vectors at any specified time were averaged (Fig. 2). For analysis of velocity profiles, the individual vectors were mapped along the width of the hyphae. Since velocity and hyphal diameter varied from one experiment to another, both velocity and location along the hyphal width were normalized (to maximal velocity and the hyphal radius, respectively). Best fits of the velocity profiles were to a parabolic model (a simplified version of the Hagen-Poiseuille equation: $v(r)=a(1-r^2)$, where $v(r)$ is the velocity at normalized radial distance r (ranging from -1 to 1) and a is a fit parameter, or to an arbitrary catenary ($v(r)=(1.544–\cosh(r))^a–b$, where a and b are fit parameters).

Modulating organelle flow. To assess as directly as possible the role of pressure gradients in driving organelle movement through the hyphae, the mycelia were placed in a chamber that allowed the extracellular osmoticum to be varied at will in separate compartments. The GFP-tagged histone strain was grown between two layers of dialysis membrane (molecular weight cut-off of 12,000—14,000) overnight at 28ºC in the dark. A section of the mycelium that included the growing edge of the colony was cut with a razor blade and carefully lifted and placed in a chamber with a cover slip window (to allow imaging) (a schematic of the setup is shown in Fig. 6a). Two beads of petroleum jelly were applied above the upper

dialysis membrane and a 22×50 mm cover slip overlaid on the petroleum jelly so that three water impermeant zones were created. Nuclei movement was imaged in the central zone with a ×10 objective on a Zeiss Axioskop fluorescent microscope. Fluorescent imaging used a filter set 15 (excitation at 546 nm; longpass emission at 590 nm) and a Hamamatsu Orca C4742-95 camera controlled by Openlab software (Improvision); images were collected at 1 second intervals. For these experiments, we selected larger trunk hypha within the mycelial network for which nuclei movement was towards the colony edge. -The nuclei were tracked for 4 sequential images and mean velocities were calculated from the three 1-second intervals. The two outer zones were filled with a buffered solution (BS) that contained (in mM): KCl (10), $CaCl_2$ (1), $MgCl_2$ (1), sucrose (133), and MES (10), pH adjusted to 5.8 with KOH. To modify the trans-hyphal pressure gradient, BS plus 500 mM sucrose was added to one of the outer compartments. The osmolarities of the solutions were 205 mOsmol for BS and 970 mOsmol for BS plus 500 mM sucrose, measured with an osmometer (5005 Osmette II, Precision Systems Inc.). The absolute magnitude of the pressure gradient between the two outer compartments can be calculated from the Van't Hoff relation ($\Delta P=RTc$, where ΔP is the pressure difference, R is the gas constant [8.314 L kPa K^{-1} mol^{-1}], T is the temperature [K] and c is the osmolarity) and the distance between the two compartment (1.5 cm): about 1200 kPa/cm. Because the dialysis membrane slows diffusive equilibration at the hyphal layer, the actual gradients will be much lower. Although we are unable to image growth at the colony edge simultaneously, we expect that the treatments would inhibit growth for at least a brief period of time based on general observations when measuring colony growth.

Statistics. Results are shown as mean ± standard deviation (sample size). Statistics and linear regressions were calculated in Excel (Microsoft). Non-linear regressions were performed in Kaleidagraph (Synergy Software).

RESULTS

To study the nature of flow in *Neurospora crassa*, we mapped the velocity vectors of organelles using confocal microscopy. The GFP-tagged histone (for imaging nuclei) and GFP-tagged calcium transporter *nca2* (for imaging vacuoles) provided us with *in situ* tools for mapping organelle movement. The MitoTracker allowed us to label mitochondria so that dual imaging of two different organelles could be done simultaneously. The vector maps of flow through a region of the hypha (an example is shown in Fig. 2) revealed that the movement of the uniformly distributed nuclei (or vacuoles) and mitochondria was consistently unidirectional and normally acropetal (towards the growing edge of the colony). This well-defined directionality was very clear a small distance behind the colony edge (within 1 cm). Further back —where anastomoses would be expected to create a more complex network—acropetal movement was less clear (especially in smaller hyphae, personal observation). Even here, uni-directional movement was consistently observed for any given hypha. For correlative analysis, the velocity vectors were averaged for each specific time interval. A total of 11 hyphae were used in analysis of mitochondria and nuclei, and 5 hyphae for mitochondria and vacuoles. The direction of flow deviated very little from parallel movement within the hyphae (Fig. 3), and plots of angles for

mitochondria and nuclei (Fig. 3a) or vacuoles (Fig. 3b) were strongly clustered at 0º as expected for unidirectional flow parallel to the hyphal walls.

Organelle velocities were strongly correlated (Fig. 4). The regression slope of the velocities of nuclei and mitochondria was nearly one (Fig. 4a). For vacuole and mitochondria velocities (Fig. 4b), vacuoles appeared to move slower than mitochondria, but even here the regression slope was close to one. It is possible that the slightly slower velocity of the vacuoles may be due to their larger size, and thus more likely to be affected by immobile elements in the cytoplasm (such as the cytoskeleton).

A hallmark of low Reynolds number flow in hyphae (Lew, 2005) is the expectation that velocity profiles of the cytoplasmic fluid will be parabolic: maximal at the center of the hypha and decreasing to zero at the hyphal walls. This relation of velocity as a function of radial distance (*v(r)*) is predicted from the Hagen-Poiseuille equation:

$$v(r) = \left(\frac{\Delta p}{l}\right)\left(\frac{1}{4\eta}\right)\left(R^2 - r^2\right)$$

where $\Delta p/l$ is the pressure gradient, η is the viscosity, R is the hyphal radius and r is the radial location. Velocity profiles were constructed for nuclei and mitochondria movement; vacuole movements were not examined due to the lower sample size (and the large size of the vacuoles). In order to fit velocity profiles, the Hagen-Poiseuille equation was simplified to the form $v(r)=a(1-r^2)$, where $a=[\Delta p/l][1/(4\eta)]$ and r —the radius— is normalized so that R is equal to 1. The predicted parabola fit the date very poorly (Fig. 5). Instead, there was a flat profile of velocity, independent of radial distance. This is probably due to the presence of high concentrations of organelles in the cytosol, resulting in "partial plug flow" (Karnis et al., 1966; see Discussion).

The close correspondence of velocities for the three organelles is strong indirect evidence of the dominant role of pressure-mediated organelle movement in the hyphae. It is unlikely that molecular motors could transport disparate organelles with such consistent velocity. Direct evidence for pressure mediation was obtained by modifying the extracellular osmoticum on either side of petroleum jelly barriers. The basic setup is shown in Fig. 6a. Hyphae were constrained to 2 dimensions by being grown between two layers of dialysis membrane. Petroleum jelly beads overlaying the upper dialysis membrane created three compartments. The two end compartments were filled with BS. After imaging for 40 seconds to establish a baseline of nuclei velocities, the solution in one of the compartments was changed to BS plus 500 mM sucrose. The effect of the addition depended on whether the solution change was made behind the colony edge (basal) or at the colony edge (apical). If the addition was basal, velocities decreased, or even reversed (Fig. 6b); if apical, velocities increased (Fig. 6c). For all experiments, the change in velocity was 2.3 ± 1.6 µm sec^{-1} (n=12). The velocity change was reversed by a return to BS after treatment with BS plus 500 mM sucrose (Fig. 6d). It is not possible to determine the actual magnitude of the trans-hyphal pressure gradient accurately because the high osmolarity solution would take time to diffuse through the dialysis membrane to the hyphae. Therefore, the overall gradient will be significantly lower than that calculated from the Van't Hoff relations for the two

compartments (see Methods). In other experiments measuring turgor, injection of a large bolus of silicon oil into a hypha causes fast cytoplasmic flow (Lew, unpublished) even though the change to the trans-hyphal pressure gradient is low relative to the high hydrostatic pressure of the hyphae (about 400–500 kPa, Lew and Nasserifar, 2009). Although we are unable to quantify the relation between the pressure gradient and flow velocity, the effect of modifying the trans-hyphal pressure gradient on cytoplasmic flow indicates clearly the role of pressure-driven flow directly.

DISCUSSION

In order to study the nature of mass flow in fungal hyphae, we tracked the movements of two different organelles simultaneously (nuclei and mitochondria, or vacuoles and mitochondria) using dual fluorescent imaging on a confocal microscope. Correlated organelle movements —both velocity and direction— provide evidentiary support for the primary role of mass flow in movements of cytoplasm in the trunk hyphae. It's important to note that movement of nuclei in a direction opposite (basipetal) to that of the normal tip-directed movement was occasionally observed near the hyphal wall, consistent with some contribution by a cytoskeleton/motor system (*cf* Ramos-García et al., 2009). But basipetal movement of individual nuclei at the wall was rare. Certainly, molecular motors have been implicated in numerous aspects of fungal growth (Steinberg, 2007), but flow can be independent of the activity of molecular motors (Lew, 2011). This idea arose from a previous report in which silicon oil was injected into the hyphae, and moved similarly to vacuoles (Lew, 2005) and warranted the more detailed exploration described here.

Using fluorescent imaging, it was possible to map the velocity profiles of nuclei and mitochondria. This allowed a direct test of the mechanism of flow. At low Reynolds number, flow through a tube is expected to be laminar, with a continuous change in shear from the immobile cell wall to the center of the hyphal tube. This will cause a gradient of velocities —highest in the center of the tube— that has a parabolic shape (the Hagen-Poiseuille equation). When data from multiple experiments are collected and normalized to maximal velocity and hyphal width, there is considerable scatter, but the data do not fit the parabolic shape predicted for laminar flow. Instead, velocity is nearly the same at the center of the hyphae and close to the cell wall. This velocity profile is consistent with low Reynolds number flow of particle suspensions (reviewed by Cox and Mason, 1971). Karnis et al. (1966) measured particle movements in tubes at low Reynolds number ($<10^{-3}$) similar to the Reynolds number of hyphal flow, about 10^{-4} (Lew, 2005). They observed a transition from a parabolic velocity profile to a 'flat-top' velocity profile when the volume fraction of particles was increased to values above about 0.18, and described the velocity profile as "partial plug flow". It was observed with both spherical and disk-shaped particles, and was more pronounced with larger particles. In hyphae, the volume fraction of organelles flowing in the hyphae is considerably higher than 0.18 (*cf* Fig. 1), and the velocity profile we observe is consistent with "partial plug flow". An intuitive explanation of the partial plug flow is that the organelles themselves affect laminar flow they disrupt shearing of the fluid from the immobile cells walls to the hyphal center causing a flat velocity profile. This would maximize the integrity of the cytoplasm continuum since all the cytoplasmic

297 components would move in tandem.
298
299 It could be argued that the coordinated movement of very different organelles is a
300 consequence of molecular motors and their transported cargo. As the cargo moves through
301 the cytoplasm, it could 'entrain' the surrounding fluid, resulting in mass flow. Such a
302 process has been invoked in cytoplasm streaming of the giant cells of the green alga *Chara*
303 (Verchot-Lubicz and Goldstein, 2010). Indeed, silicon oil droplets injected into the
304 cytoplasm of *Chara* move at the same rate as visible cargo, regardless of the oil droplet size
305 (from 30 to 300 micron diameters) (Cross and Lew, unpublished). Even in small plants
306 cells, it has been suggested that entrained mass flow occurs (Esseling et al., 2008). The
307 movement of green fluorescence protein (free GFP) in cytoplasmic strands was measured
308 using fluorescence bleaching recovery and found to be affected by treatments with a myosin
309 inhibitor, and correlated with the movement of organelles, providing support for cytosol
310 entrainment. The situation for plant cells is different from that of fungal hyphae, which are
311 cytoplasm-rich and do not exhibit the relatively narrow trans-vacuolar cytoplasmic strands
312 common to plant cells. The existence of cytosol entrainment in plants would impact on one
313 proposed function for cytoplasmic streaming in plants: higher fluxes (either uptake or
314 secretion) to and from the streaming organelles (Pickard, 2006) because of a thinner
315 diffusion zone in the absence of cytosol entrainment. This would allow the moving
316 organelles to interact with a larger volume of the surrounding cytosol. If entrained cytosol
317 moved with the organelle, it would create a thicker diffusion zone and limit fluxes. In fungi,
318 the typically acropetal movement of cytoplasm apparently fulfills a different role of
319 supplying cytoplasm to the ever-expanding hyphal tips.
320
321 Different lines of evidence suggest that cytosol entrainment by the activity of molecular
322 motors is unlikely in fungal hyphae. Nuclei move towards the growing edge of the fungal
323 colony even in strains with defective molecular motors (Ramos-García et al., 2009). By
324 directly modifying the trans-hyphal pressure gradient and showing it has rapid effects on
325 nuclei movements, we provide direct evidence for the alternative explanation —pressure-
326 mediated flow. Addition of external osmoticum basal to the colony edge causes water flow
327 out of nearby hyphae, creating a basopetal pressure gradient in the hyphal tubes. This
328 caused the velocity of nuclei movement towards the colony edge to slow down or even
329 reverse. Addition of external osmoticum at the colony edge causes water flow out of the
330 tips, creating an acropetal pressure gradient in the hyphal tubes. This caused an increase in
331 the velocity of nuclei movement towards the colony edge. Both effects can be attributed to
332 changes in the pressure gradients within the hyphal network of the colony. The nature of the
333 mass flow in the hyphal tubes is in some ways analogous to mass flow in phloem of higher
334 plants, although the physical mechanisms causing mass flow in phloem are more complex
335 than pressure-driven flow alone (Knoblauch and Peters, 2010), perhaps similar to the role of
336 the vacuolar network in nutrient translocation in the more complex architecture of the
337 Basidiomycetes (Darrah et al., 2006). Some aspects of the physical mechanisms of osmotic-
338 pressure-driven translocation (and flow of particle suspensions) may be best addressed in
339 micro-fluidic model systems (Jensen et al., 2009).
340
341 In summary, pressure-driven mass flow dominates organelle movements in *Neurospora*
342 *crassa* hyphae. Because of the high concentrations of organelles in the cytosol, the

movement is best described as “partial plug flow”. The long distance mode of pressure-driven translocation should complement the short distance transport mediated by the cytoskeleton.

Acknowledgements. We thank Kevin Cross for discussions on hydrodynamics and silicon oil injections into *Chara*, and Patricia Lakin-Thomas for her feedback as the research progressed. The research was funded by the Natural Sciences and Engineering Research Council of Canada (RRL) and RAY (Research at York) (AA).

REFERENCES

Bleichrodt, R., Vinck, A., Krijgsheld, P., van Leeuwen, M. R., Dijksterhuis, J. & Wösten H. A. (2013). Cytosolic streaming in vegetative mycelium and aerial structures of *Aspergillus niger*. *Stud Mycol* **74**, 31–46.

Bebber, D. P., Hynes, J., Darrah, P. R., Boddy, L. & Fricker, M. D. (2007). Biological solutions to transport network design. *Proc R Soc B* **274**, 2307–2315.

Bowman, B. J, Draskovic, M., Freitag, M. & Bowman, E. J. (2009). Structure and distribution of organelles and cellular location of calcium transporters in *Neurospora crassa*. *Eukaryot Cell* **8**, 1845–1855.

Cox, R. G. & Mason, S. G. (1971). Suspended particles in fluid flow through tubes. *Ann Rev Fluid Mech* **3**, 291–316.

Darrah, P. R., Tlaka, M., Ashford, A., Watkinson, S. C. & Fricker, M. D. (2006). The vacuole system is a significant intracellular pathway for longitudinal solute transport in Basidiomycete fungi. *Eukaryot Cell* **5**, 1111–1125.

Esseling. A., Houtman, D., Van Lammeren, A. A. M., Eiser, E. & Emons, A. M. C. (2008). Hydrodynamic flow in the cytoplasm of plant cells. *J Microscopy* **231**, 274–283.

Freitag, M., Hickey, P. S., Raju, N. B., Selker, E. U. & Read, N. D. (2004). GFP as a tool to analyze the organization dynamics and function of nuclei and microtubules in *Neurospora crassa*. *Fungal Genet Biol* **41**, 897–910.

Fricker, M. D., Lee, J. A., Bebber, D. P., Tlalka, M., Hynes, J., Darrah, P. R., Watkinson, S. C. & Boddy, L (2007). Imaging complex nutrient dynamics in mycelial networks. *J Microscopy* **231**, 317–331.

Jennings, D. H. (1987). Translocation of solutes in fungi. *Biol Rev* **62**, 215–243.

Jensen, K. H., Lee, J., Bohr, T. & Bruus, H. (2009). Osmotically driven flows in microchannels separated by a semipermeable membrane. *Lab Chip* **9**, 2093–2099.

Karnis, A., Goldsmith, H. L. & Mason, S. G. (1966). The kinetics of flowing dispersions. I. Concentrated suspensions of rigid particles. *J Colloid Interface Sci* **22**, 531–553.

Knoblauch, M. & Peters, W. S. (2010). Münch, morphology, microfluidics — our structural problem with phloem. *Plant Cell Environ* **33**, 1439–1452.

Lew, R. R. (2005). Mass flow and pressure-driven hyphal extension in *Neurospora crassa*. *Microbiology* **151**, 2685–2692.

Lew, R. R. (2011). How does a hypha grow? The biophysics of pressurized growth in fungi. *Nat Rev Microbiol* **9**, 509–518.

Lew, R. R. & Nasserifar, S. (2009). Transient responses during hyperosmotic shock in the filamentous fungus *Neurospora crassa*. *Microbiology* **155**, 903–911.

Levina, N. N. & Lew, R. R. (2006). The role of tip-localized mitochondria in hyphal growth. *Fungal Genet Biol* **43**, 65–74.

Luck, D. J. L. (1963). Formation of mitochondria in *Neurospora crassa*: A quantitative radioautographic study. *J Cell Biol* **16**, 483–499.

McCluskey, K., Wiest, A. & Plamann, M. (2010). The Fungal Genetics Stock Center: repository for 50 years of fungal genetics research. *J Bioscience*s **35**, 119–126.

Mourino-Perez, R. R., Roberson, R. W. & Bartnicki-Garcia, S. (2006). Microtubule dynamics and organization during hyphal growth and branching in *Neurospora crassa*. *Fungal Genet Biol* **43**, 389–400.

Pickard, W. F. (2006). Absorption by a moving spherical organelle in a heterogenous cytoplasm: Implications for the role of trafficking in a symplast. *J Theor Bio*l **240**, 288–301.

Ramos-García, S. L., Roberson, R. W., Freitag, M., Bartnicki-García, S. & Mouriño-Pérez, R. R. (2009). Cytoplasmic bulk flow propels nuclei in mature hyphae of *Neurospora* crassa. *Eukaryot Cell* **8**, 1880–1890.

Rasband, W. S. ImageJ, U. S. National Institutes of Health, Bethesda, Maryland, USA, http://imagej.nih.gov/ij/, 1997-2013.

Riquelme, M., Roberson, R. W., McDaniel, D. P. & Bartnicki-García, S. (2002). The effects of ropy-1 mutation on cytoplasmic organization and intracellular motility in mature hyphae of *Neurospora crassa*. *Fungal Genet Biol* **37**, 171–179.

Roper, M., Simonin, A., Hickey, P. C., Leeder, A. & Glass, N. L. (2013) Nuclear dynamics in a fungal chimera. *Proc Natl Acad Sci USA* **110**. 12875-12880.

Simonin A., Palma-Guerrero J., Fricker, M. & Glass, N. L. (2012). Physiological

significance of network organization in fungi. *Eukaryot Cell* **11**, 1345–1352.

Steinberg, G. (2007). Hyphal growth: a tale of motors, lipids and the spitzenkörper. *Eukaryot Cell* **6**, 351–360.

Verchot-Lubicz, J. & Goldstein, R. (2010). Cytoplasmic streaming enables the distribution of molecules and vesicles in large plant cells. *Protoplasma* **240**, 99–107.

Vogel, H. J. (1956). A convenient growth medium for *Neurospora*. *Microbial Genetics Bulletin* 13, 42–46.

Figure 1. Image enhancement and organelle tracking. (a). Examples of (from left to right) fluorescence images of mitochondria, nuclei and vacuoles (arrow). Upper panels are the original images, lower panels are processed with Gaussian filtering and linear contrast stretch using ImageJ (Rasband, 2012). In all cases, clearly delineated organelles were selected for tracking. (b). Example of tracking a nucleus. The x,y coordinates of the nucleus (red dots) are tracked for 3 sequential images (taken at 1 second intervals). (c). The (x,y) coordinates for the three sequential images (overlaid in a single image) were transformed into an average velocity and direction for the two 1-second intervals. The average velocity (v, in µm s^{-1}) was calculated as $v = \sqrt{v_x^2 + v_y^2}$ where v_x is the average velocity in the x-direction ($v_x = \frac{(x_3 - x_2) + (x_2 - x_1)}{2}$) and v_y is the average velocity in the y-direction ($v_y = \frac{(y_3 - y_2) + (y_2 - y_1)}{2}$). The direction (angle) of growth was calculated as the average of $\tan^{-1}\left(\frac{y_2 - y_1}{x_2 - x_1}\right)$ and $\tan^{-1}\left(\frac{y_3 - y_2}{x_3 - x_2}\right)$. Individual flow vectors as organelles moved through the region of the hyphae that was being imaged are shown in Fig. 2. Bars = 10 µm.

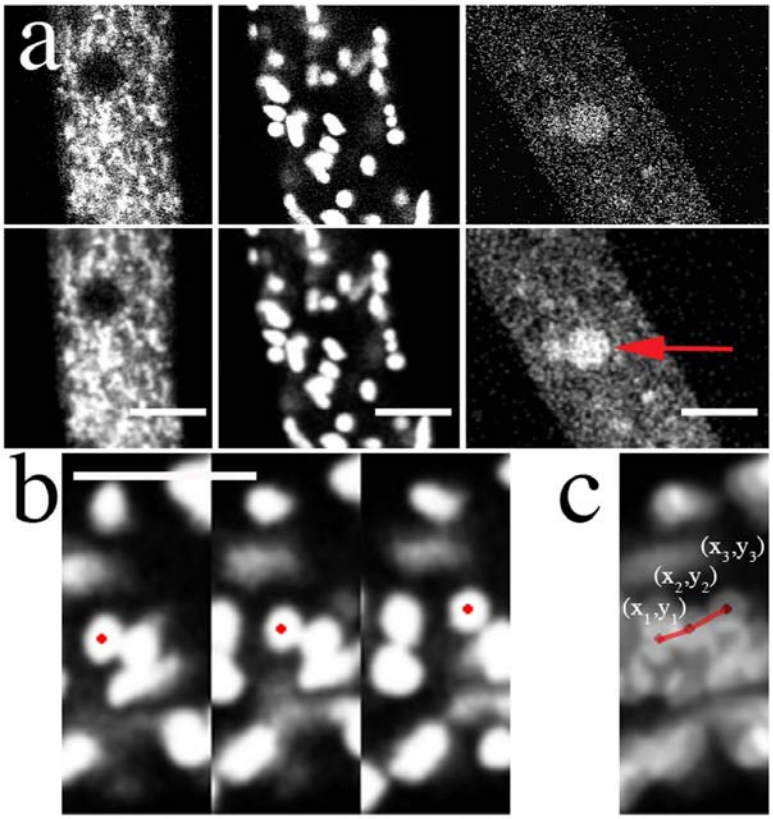

Figure 2. Examples of flow vectors for nuclei and mitochondria (a) and vacuoles and mitochondria (b). The y-axis represents the width of the hyphae and the x-axis represents time. The vectorial movement of the organelles was measured as they moved through the imaged region of the hypha over time. The vectors are centered on the midpoint of the 2-second interval in which they were measured (Fig. 1). The length of the vectors represents the magnitude of the organelle velocity, the orientation represents the angle of movement, arrowheads indicate the direction of movement. Note that the same organelle could be measured in successive 2-second time intervals (about 10 nuclei and 8 mitochondria were measured in (a) at each time interval). For further analysis of the correlations between the movements of the two organelles (Figs. 3 and 4), the organelle vectors at each time interval were averaged.

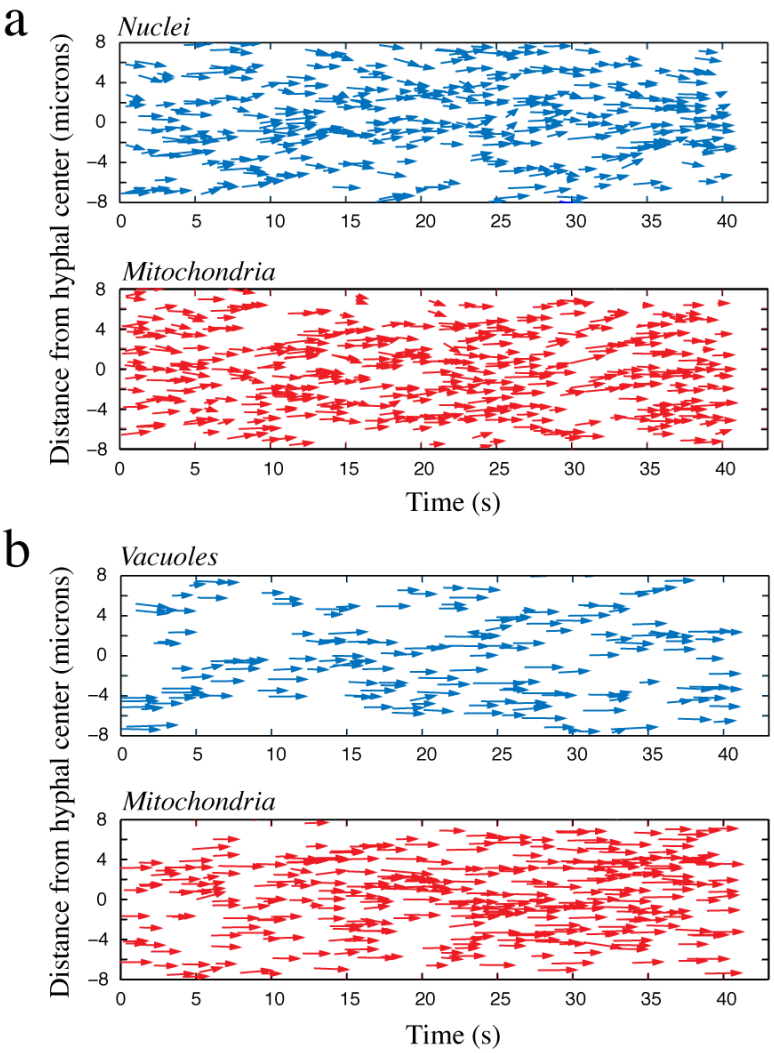

Figure 3. Flow vectors for nuclei and mitochondria (a) and vacuoles and mitochondria (b). Each point in the plot represents the correlation between the velocity of the nuclei and mitochondria (or vacuole and mitochondria) in the same hyphal region and time-frame of 2 seconds. The angles and velocities are plotted in the upper graphs, and correlations of angles in the lower graphs. There is a close correspondence of direction for the three organelles.

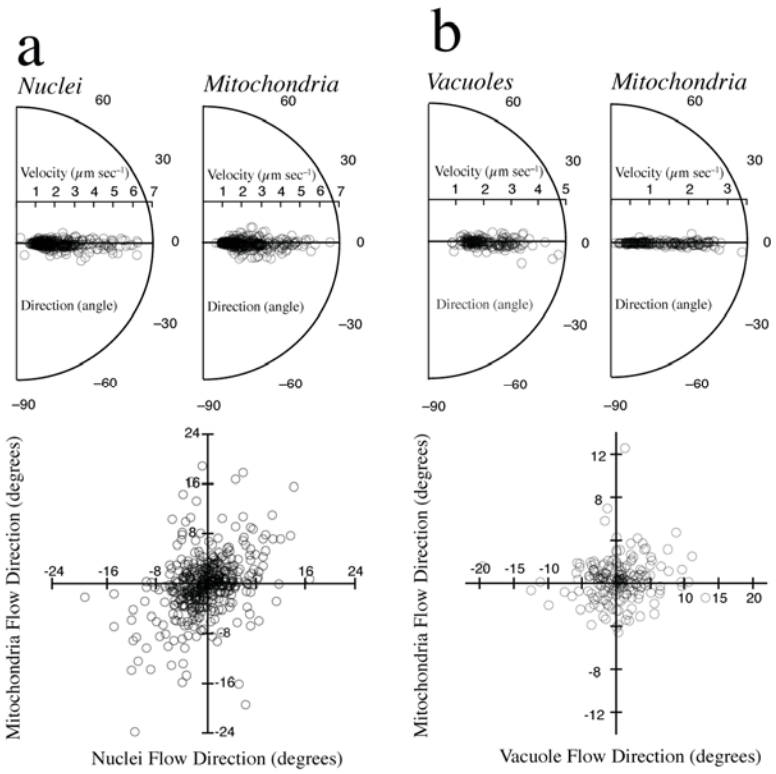

Figure 4. Correlation analysis of organelle velocities in the hyphae of *Neurospora crassa*. Each point in the plot represents the correlation between the velocity of the nuclei and mitochondria (or vacuole and mitochondria) in the same hyphal region and time-frame of 2 seconds. Both linear regression fits (black lines) and a line with a slope of one (gray lines) are shown in each graph. (a). Nuclei and mitochondria. The mean velocities (μm s^{-1}) were 1.97±1.10 for nuclei, and 2.07±1.04 (n=440) for mitochondria. The mean velocities were not significantly different on the basis of a 2-tail t-test (P=0.154). The regression fit indicates a close correspondence of velocities (a slope of 0.96). (b). Vacuoles and mitochondria. The mean velocities (μm s^{-1}) were 2.08±0.72 for vacuoles, and 2.22±0.72 (n=200) for mitochondria. The mean velocities were not significantly different on the basis of a 2-tail t-test (P=0.055). However, the regression fit suggests that vacuoles moved slightly slower than mitochondria (a slope of 0.76). Data are compiled from independent experiments: 11 hyphae for nuclei and mitochondria, and 5 hyphae for vacuoles and mitochondria.

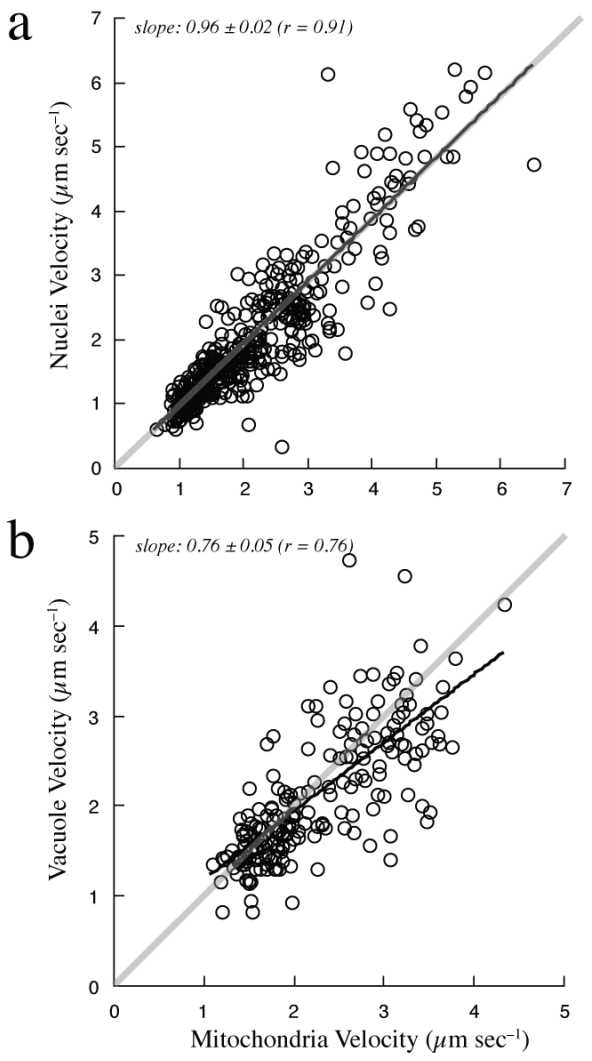

Figure 5. Velocity profiles for mitochondria (a) and nuclei (b). The individual velocities of all measurements are shown (mitochondria, n=3784; nuclei, n=4007). They were normalized to the maximal velocity for each hypha. Radial distance is normalized to each hyphal radius. The average hyphal diameter was 18.4 ± 1.9 µm (n=11) (range: 15.0—20.8 µm). Open circles are the mean velocities for binned normalized radial distances of 0.1 (except mitochondria at the walls of the hyphae, which were binned from ±0.8 to ±1 to increase the sample size near the cell walls). Best fits are to a Hagen-Poiseuille model (*a*), which predicts a parabolic profile with maximal velocity at the center of the hyphae, and an arbitrary catenary function (*b*) that emphasizes that the velocity profile is much flatter than that predicted for Hagen-Poiseuille mass flow.

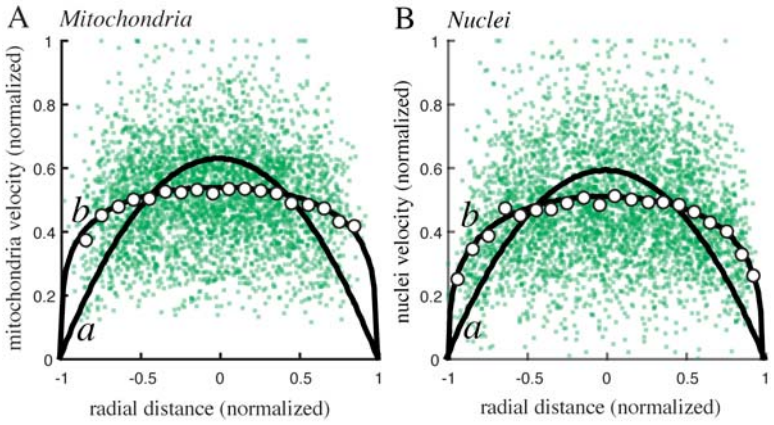

Figure 6. Osmotically-driven organelle flow. (a). The cultures were grown between two layers of dialysis membrane to ensure a flat geometry. Sections of the mycelium (including the growing colony edge) were cut and carefully placed in a holder with a central circle with a cover slip window. Two beads of petroleum jelly were placed about 0.3 cm apart, and a cover slip placed on top, such that three water impermeant zones were created. The two outer zones were filled with BS; the inner zone was left empty. Nuclei movements were imaged by tracking them for three 1-second intervals, followed by changes in the osmolarity of one of the two outer chambers, and continued imaging of nuclei movement. In (b) and (c), representative experiments are shown, from experiments with little effect (upper panels) to experiments with rapid and large effects on organelle velocity (lower panels). (b). Additions of BS plus 500 mM sucrose basal caused water outflow form the hyphae, resulting in a decrease (or even reversal) in the normally acropetal nuclei movement. (c). Additions of the osmoticum on the apical side (where the colony edge is located) caused an increase in nuclei movements towards the colony edge. (d). An experiment demonstrating reversibility of the effect of osmoticum. At time 40 seconds, BS was replaced with BS plus 500 mM sucrose then replaced with BS alone at 500 seconds (horizontal bar), reversing the change in velocity caused by BS plus 500 mM sucrose.

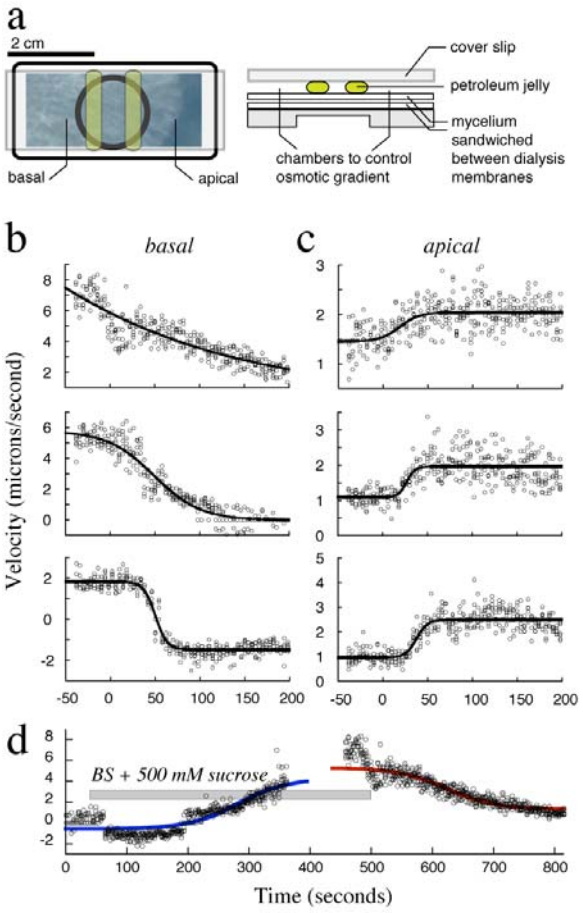

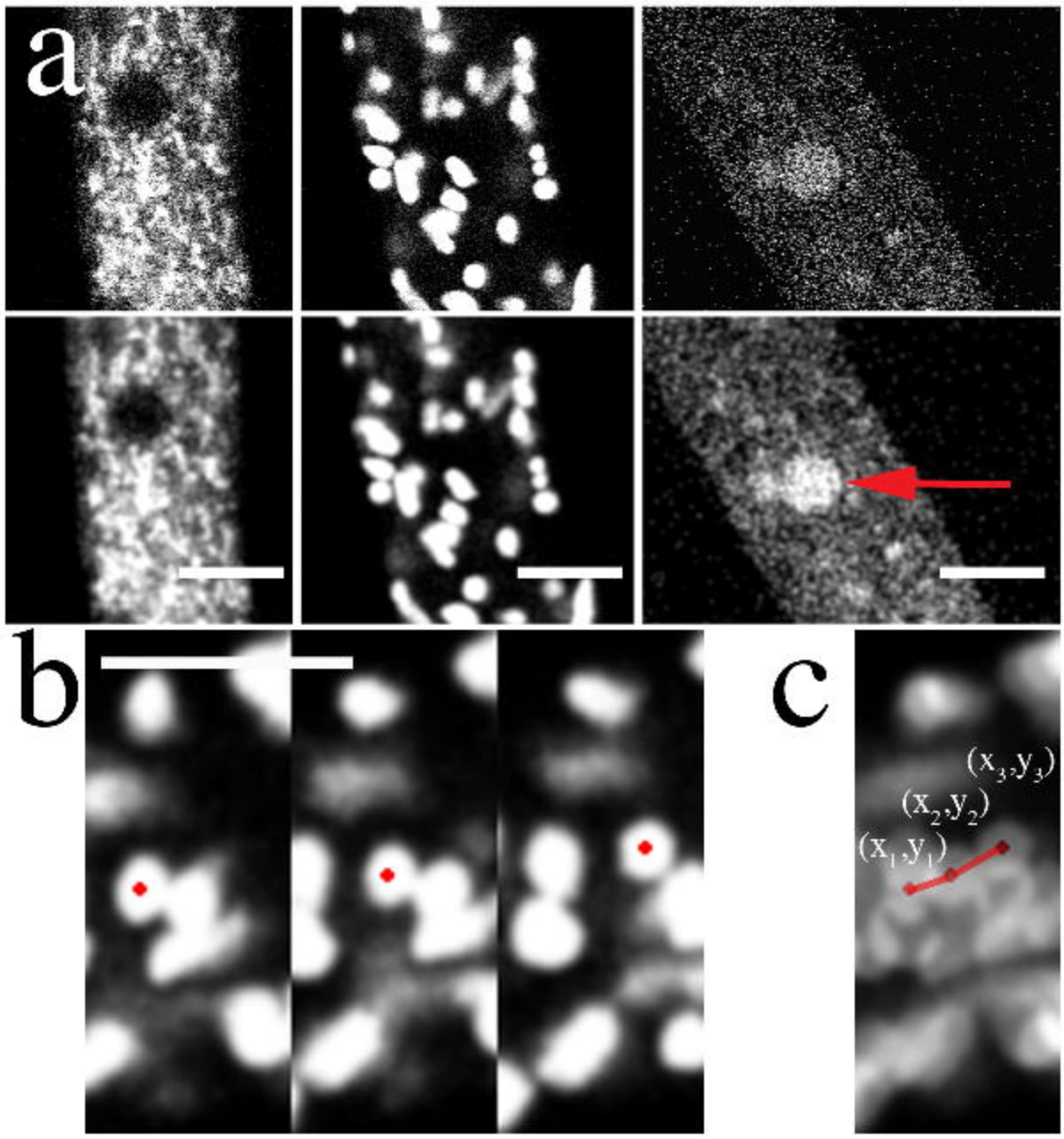
a
b
c
(x_3,y_3)
(x_2,y_2)
(x_1,y_1)

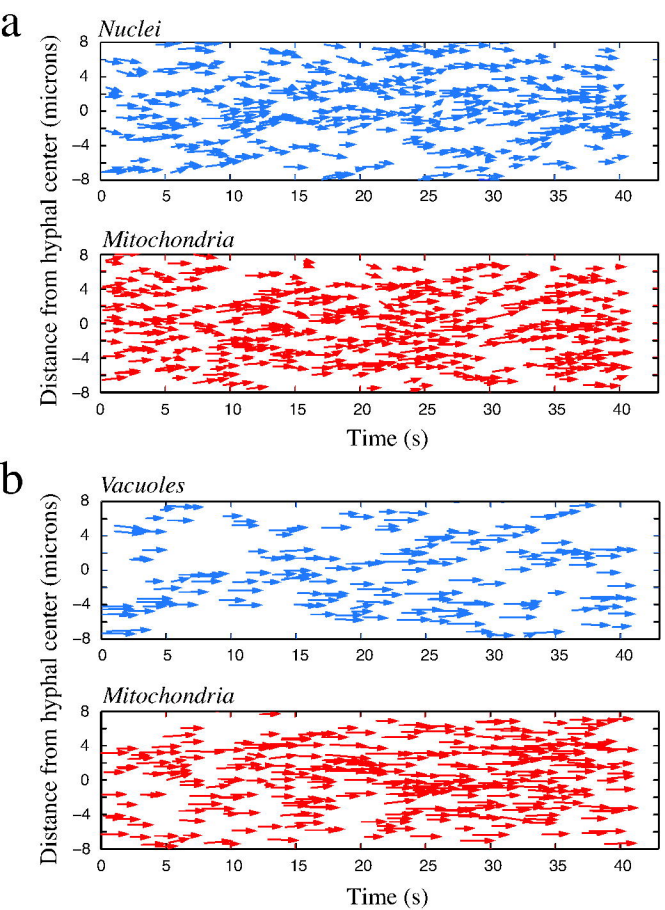
a
Nuclei
Mitochondria
Distance from hyphal center (microns)
Time (s)
b
Vacuoles
Mitochondria
Distance from hyphal center (microns)
Time (s)

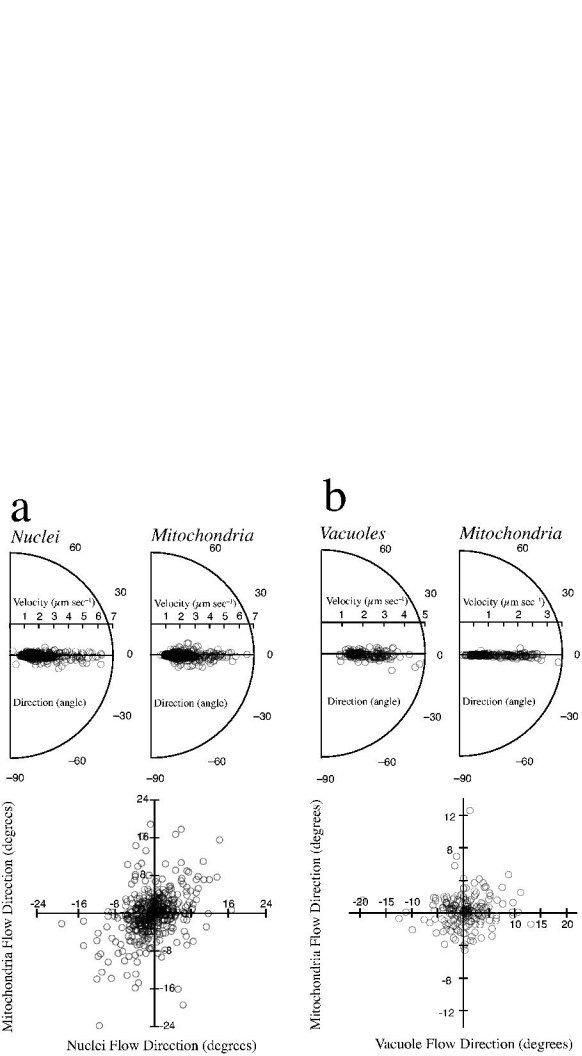
a
Nuclei
Mitochondria
60
30
0
−30
−60
−90
Velocity (μm sec⁻¹)
1 2 3 4 5 6 7
Direction (angle)
24
16
8
-8
-16
-24
Mitochondria Flow Direction (degrees)
Nuclei Flow Direction (degrees)
b
Vacuoles
Mitochondria
1 2 3 4 5
1 2 3
12
8
-8
-12
-20 -15 -10 10 15 20
Vacuole Flow Direction (degrees)

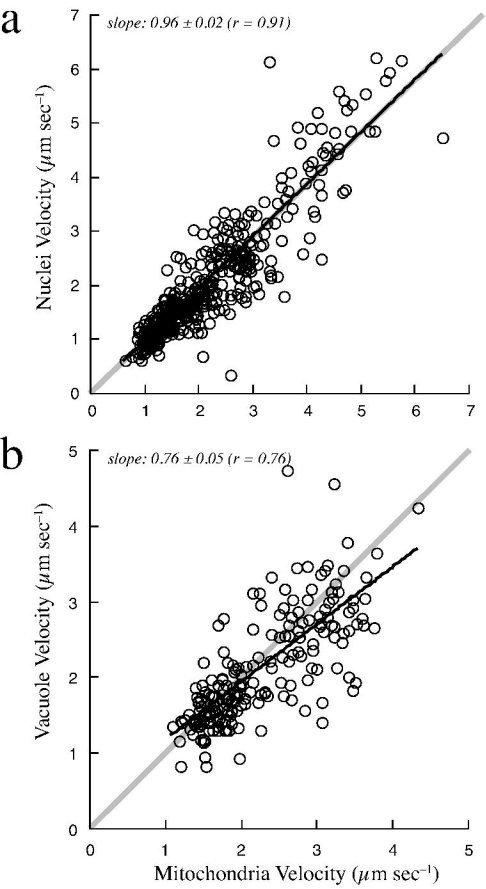
a
slope: 0.96 ± 0.02 (r = 0.91)
Nuclei Velocity (μm sec⁻¹)
0
1
2
3
4
5
6
7
b
slope: 0.76 ± 0.05 (r = 0.76)
Vacuole Velocity (μm sec⁻¹)
Mitochondria Velocity (μm sec⁻¹)

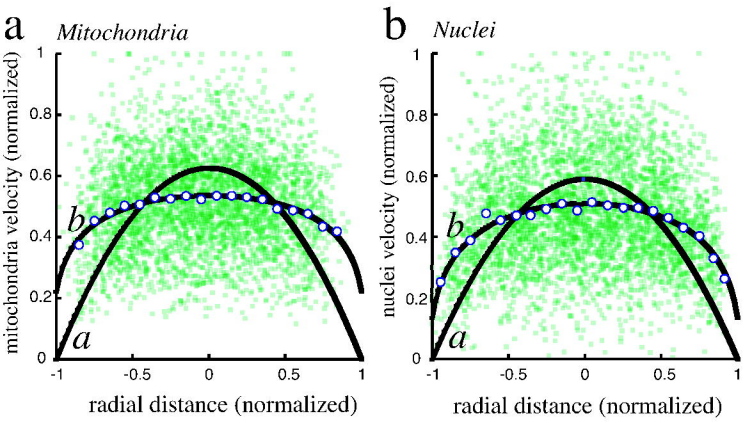
a
Mitochondria
mitochondria velocity (normalized)
1
0.8
0.6
0.4
0.2
0
b
a
-1
-0.5
0
0.5
1
radial distance (normalized)
b
Nuclei
nuclei velocity (normalized)
1
0.8
0.6
0.4
0.2
0
b
a
-1
-0.5
0
0.5
1
radial distance (normalized)

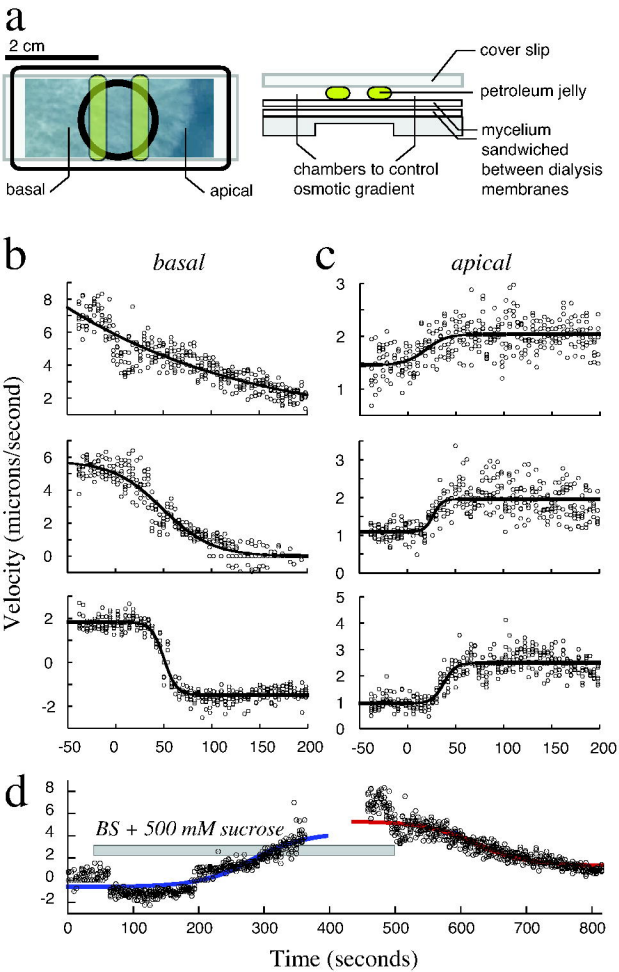
a
2 cm
basal
apical
cover slip
petroleum jelly
mycelium
sandwiched
between dialysis
membranes
chambers to control
osmotic gradient
b
basal
c
apical
Velocity (microns/second)
d
BS + 500 mM sucrose
Time (seconds)